MECHANICAL BEHAVIOR OF HIGH-DENSITY POLYETHYLENE REINFORCED WITH GRAPHENE NANOPLATELETS AND JUTE FABRIC

COMPORTAMIENTO MECÁNICO DEL POLIETILENO DE ALTA DENSIDAD REFORZADO CON NANOPLAQUETAS DE GRAFENO Y TEJIDO DE JUTE

COMPORTAMENTO MECÂNICO DO POLIETILENO DE ALTA DENSIDADE REFORÇADO COM NANOPLATAS DE GRAFENO E TECIDO DE JUTE

ULISSES OLIVEIRA COSTA, MSc. | Instituto Militar de Engenharia (IME), Brasil
WENDELL BRUNO ALMEIDA BEZERRA, Dr. | Instituto Militar de Engenharia (IME), Brasil
NOEMI RAQUEL CHECCA HUAMAN, PhD. | Centro Brasileiro de Pesquisas Físicas (CBPF), Brasil
SERGIO NEVES MONTEIRO, Dr. | Instituto Militar de Engenharia (IME), Brasil
WAGNER ANACLETO PINHEIRO, Dr. | Instituto Militar de Engenharia (IME), Brasil
LUCIO FABIO CASSIANO NASCIMENTO, Dr. | Instituto Militar de Engenharia (IME), Brasil

ABSTRACT

Owing to sustainable characteristics, natural lignocellulosic fibers (FNLs) and graphene nanoplatelets (GNP)-reinforced composites are currently seeing applications in a wide range of industrial fields. Thus, in the present work, the mechanical, and flexural properties of high-density polyethylene (HDPE) reinforced with 0, 0.10, 0.25, and 0.50 wt.% of GNP and 50 vol.% of jute fabric were investigated and statistically validated through ANOVA and the Tukey test. The extrusion process followed by hot pressing resulted in films of GNP-reinforced HDPE nanocomposites that were used to fabricate the jute fabric-reinforced composite plates. In particular, the Jute/HDPE/0.25%GNP composite outperformed the strength of those described in the literature, even some with higher GNP. Enhancements of 38% were observed for the composite's flexural modulus as compared to the GNP-free Jute/HDPE composite. Regarding the tensile properties, the ductility of the Jute/HDPE/0.25%GNP was increased by 112% when compared to the Jute/HDPE. Moreover, the toughness of the Jute/HDPE/0.25%GNP was 161% superior to the Jute/HDPE composite. SEM analysis of the fracture surfaces showed that, as GNP concentration rises, the fracture mechanisms change from a shear band to a complex mixture of fibrillation, tearing, and crazing. Consequently, the results reveal the novel Jute/HDPE/0.25%GNP nanocomposite as a promising material for engineering applications.

KEYWORDS

Nanocomposite; Jute fabric; Graphene nanoplatelet; High-density polyethylene.

http://dx.doi.org/10.29183/2447-3073.MIX2023.v9.n3.50-65
ISSN: 2447-0899 (IMPRESSA) | 2447-3073 (ONLINE)

RESUMEN

Debido a sus características sostenibles, las fibras lignocelulósicas naturales (FLN) y los compuestos reforzados con nanoplaquetas de grafeno (GNP) están siendo utilizados en una amplia gama de campos industriales. En este trabajo, se investigaron las propiedades mecánicas y de flexión del polietileno de alta densidad (HDPE) reforzado con 0%, 0.10%, 0.25% y 0.50% en peso de GNP combinado con 50% en volumen de tejido de yute. Se validaron estadísticamente las propiedades mecánicas y flexurales del polietileno de alta densidad (HDPE) reforzado con GNP y tejido de yute utilizando ANOVA y la prueba de Tukey. El proceso de extrusión seguido del prensado en caliente dio como resultado películas de nanocompuestos de HDPE reforzados con GNP que se utilizaron para fabricar las placas compuestas reforzadas con tejido de yute. En particular, se observó que el compuesto Jute/HDPE/0.25%GNP superó la resistencia de los compuestos descritos en la literatura, incluso algunos con mayor concentración de GNP. Se observaron mejoras del 38% en el módulo de flexión del compuesto en comparación con el compuesto Jute/HDPE sin GNP. En cuanto a las propiedades de tracción, se incrementó la ductilidad del Jute/HDPE/0.25%GNP en un 112% en comparación con el Jute/HDPE. Además, la tenacidad del compuesto Jute/HDPE/0.25%GNP fue un 161% superior a la del compuesto Jute/HDPE. El análisis SEM de las superficies de fractura mostró que, a medida que aumenta la concentración de GNP, los mecanismos de fractura cambian de una banda de corte a una mezcla compleja de fibrilación, desgarro y agrietamiento. En consecuencia, los resultados revelan que el novedoso nanocompuesto Jute/HDPE/0.25%GNP es un material prometedor para aplicaciones de ingeniería.

PALABRAS CLAVE

Nanocompuesto; tela de Jute; nanoplaquetas de grafeno; Polietileno de alta densida.

RESUMO

Devido às características sustentáveis, as fibras lignocelulósicas naturais (FNLs) e os compósitos reforçados com nanoplaquetas de grafeno (GNP) estão atualmente tendo aplicações em uma ampla gama de campos industriais. Assim, no presente trabalho, foram investigadas as propriedades mecânicas e de flexão do polietileno de alta densidade (PEAD) reforçado com 0, 0,10, 0,25 e 0,50% em peso de GNP combinado com 50% em volume de tecido de juta. Em particular, o compósito JutaJuta/HDPE/0,25%GNP superou a resistência daqueles descritos na literatura, mesmo para alguns com maior GNP. Melhorias de 38% foram observadas para o módulo de flexão do compósito em comparação com o compósito de juta/HDPE livre de GNP. Com relação às propriedades de tração, a ductilidade da Juta/HDPE/0,25%GNP foi aumentada em 112% quando comparada à Juta/HDPE. Além disso, a tenacidade do compósito Juta/HDPE/0,25%GNP foi 161% superior à do compósito Juta/HDPE. A análise SEM das superfícies de fratura mostrou que, à medida que a concentração de GNP aumenta, os mecanismos de fratura mudam de uma banda de cisalhamento para uma mistura complexa de fibrilação, rasgo e fissura. Consequentemente, os resultados revelam o novo nanocompósito Juta/HDPE/0,25%GNP como um material promissor para aplicações em engenharia.

PALAVRAS CHAVE

Nanocompósito; Tecido de juta; Nanoplaqueta de grafeno; Polietileno de alta densidade.

1.INTRODUCTION

Natural lignocellulosic fibers (NLFs) have been gaining attention from researchers around the world as reinforcement for engineering applications in the past decades [1-5]. They find applications in polymer matrix composites, particularly in the automobile industry [6,7], packaging [8], biomass [9], as well as building materials [10,11]. The potential of NLF composites has been associated with several of their inherent advantages when compared to synthetic fibers such as low cost, low density, comparable specific tensile properties, non-abrasion to equipment, non-irritation to the skin, reduced energy consumption, lower health risk, renewability, recyclability, and biodegradability [11]. In fact, polymer matrix composites reinforced with NLFs proved to be as efficient as those produced with synthetic fibers, especially fiberglass [12]. Furthermore, in recent years it has been reported that NLF composites can even successfully replace aramid fiber or fabric (Kevlar™) in ballistic protection applications with equal or even greater efficiency [13-20].

Regarding polymeric composites reinforced with NLFs, they could be cheaper, stronger, and more environmentally friendly, but the potential of NLFs for polymeric composites has not yet been fully explored. As for the matrix, there are three options widely available: thermoset, rubber, and thermoplastic. According to Gowda *et al*. [21], the main thermoplastics used as matrices for composites are nylon, cellulose acetate, polystyrene (PS), polypropylene (PP), polyethylene (PE), polycarbonate (PC), polyvinyl chloride (PVC), polyether-ether ketone (PEEK), and acrylonitrile-butadiene-styrene (ABS). Among these, the PE composites, more specifically the high-density polyethylene composites (HDPE), offer low cost and ease of processing (via injection molding or extrusion) [22]. Several authors have reported the use of natural fibers as reinforcement in HDPE composites such as corn [23], PALF [24], kenaf [25], sugarcane bagasse [26], and coconut [27,28]. In all cases, the composites showed improved tensile, bending, impact, and thermal properties. These properties might be further improved in novel nanocomposites.

Nanocomposites, notably those based on graphene, have distinguished themselves from composites consisting merely of NLFs and polymeric matrices due to their even more optimized characteristics and diversity of reinforcements [29,30]. Due to its amazing capabilities, graphene has attracted a great deal of interest ever since it was discovered and industrially produced [29]. Graphene has become a more desirable alternative as a reinforcing phase in polymeric materials, due to the possibility to be produced in vast quantities from inexpensive graphite [31-34]. High-ratio graphene nanoplatelets (GNP), which can be thought of as small stacks of graphene sheets with thicknesses varying from 1 to 20 nm, are produced when graphite expands. In theory, the large surface area of GNPs is a key factor for nucleation during polymer crystallization. Consequently, this can cause a considerable increase in thermal, mechanical, and physical properties [30,33,34].

Jute fiber (*Corchorus capsularis*) stands out among the many NLFs with potential application in engineering. This fiber is one of the best-known and most studied NLFs in the world, as well as one of the cheapest and strongest [35]. Jute fiber has traditionally been used to make bags, fabrics, rugs, yarns, and ropes. The automotive, construction, and packaging industries have also used this fiber as a reinforcing material [36-39]. In addition, compared to glass, carbon, and aramid fibers, jute fiber has a lower density and is lighter, with higher specific strength and stiffness. Some important physical and mechanical properties of jute fiber are as follows: density 1.3-1.46 g cm-3, elongation 1.5%-1.8%, tensile strength () 393-800 MPa, specific tensile strength () 302-547 MPa/gcm^3, Young's modulus (E) 10-30 GPa and specific Young's modulus () 8-20.5 GPa/gcm^3 [35,40].

Consequently, polymer matrix composites reinforced with jute fiber and GNP offer certain essential sustainability qualities. Such as the use of more environmentally friendly materials, such as jute fiber, and the manufacturing of GNP that does not result in solvent discharge in the environment. There is also the added value to the product, which was formerly utilized for handicrafts. As a result, the novel nanocomposite will be able to have nobler uses, such as engineering applications, and shift the economy more forcefully towards more sustainable materials. Thus, in this work, for the first time, the mechanical and flexural properties of jute fabric/GNP-reinforced HDPE nanocomposites were investigated.

2. MATERIAL AND METHODS

2.1 Jute Fabric

The jute fabric was purchased from the company Sisalsul, Figure 1, based in São Paulo, Brazil. The fiber density was

assumed to be ~1.3 g/cm^3, according to Monteiro *et al.* [3].

(A) (B)

Figure 1: Jute: (a) Plant (*Corchorus Capsulares*); (b) fabric.
Source: Author (2023).

The jute fabric with a simple weave was cut to the dimensions of 120 x 120 mm and properly dried in an oven at 60 °C for 24 h.

2.2. High-density polyethylene (HDPE)

High-density polyethylene (HDPE), grade HE150, was purchased from Braskem, São Paulo, Brazil, in the form of pellets. HDPE density was considered to be 0.948 g/cm^3, according to the product specification provided by Braskem. The HE150 resin is specially developed for the monofilament extrusion process. Commonly applied for the extrusion of orientated structures, it exhibits a low level of gel and an excellent mix of processability, reliability, and stability.

2.3. Graphene nanoplatelets (GNPs)

UCSGraphene, Caxias do Sul, Brazil, provided the graphene nanoplatelets (GNP). This material was supplied as a powder with particles made up of 10 to 50 layers of graphene. Used to strengthen the HDPE matrix in nanocomposites with 0, 0.10, 0.25, and 0.50 wt.% of GNP.

2.4. Nanocomposites fabrication

Initially, the GNP powder was mixed with HDPE through mechanical agitation to produce a concentrate. Subsequently, the GNP/pellets mixture was processed into four GNP weight fractions, corresponding to 0.10, 0.25, and 0.50 wt.%. in an interpenetrating, co-rotating, twin-screw extruder Tecktril, model DCT-2. According to Escocio *et al*. [41], the ideal extrusion conditions were set as: screw rotation of 300 rpm; feeder rotation of 15 rpm; temperature in the processing zones: first: 90 °C; second to fifth: 140 °C; sixth to ninth: 160 and 180 °C.

Then, from each fraction of HDPE/GNP, 300 µm-thick films were produced by hot compression molding at 150 °C, using a heat press. As one can see in Figure 2, to produce the nanocomposite plates, a laminate pattern was used, in which the fabric layers were alternately arranged with polymeric films. Thus, to reach the condition of 50 vol.% of reinforcement in the polymeric matrix, based on the methodology of Tomasi Tessari *et al*. [42], 20 layers of jute fabric were used and, consequently, 21 layers of HDPE films.

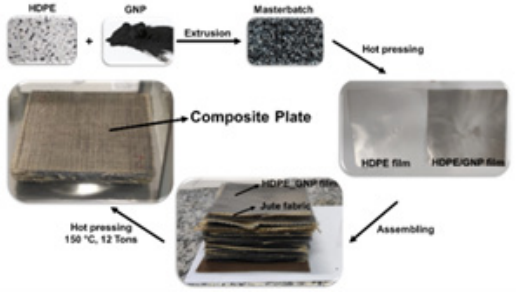

Figure 2: Scheme of the fabrication of the composite plates.
Source: Author (2023).

During the processing, the pressure was increased by one ton during 1 min for each new pressure step and 30 s of degassing. This process was repeated until reaching a pressure of 12 tons. Finally, cooling was performed at room temperature resulting in the composite plates denotated as: Jute/HDPE, Jute/HDPE/0.10%GNP, Jute/HDPE/0.25%GNP, and Jute/HDPE/0.50%GNP. Each plate had dimensions of 120 x 120 x 10 mm. The density of the nanocomposite plates was determined using the Arquimedes test and was validated by geometric measurements to be 0.92±0.031 g/cm^3.

2.5. Tensile test

The tensile tests were performed at the Mechanical Testing Laboratory at PUC-Rio, Rio de Janeiro, Brazil, using an INSTRON 3365 universal machine. The test speed and cell load parameters were 2 mm/min and 10 KN, respectively. Seven samples were cut manually with a bandsaw to the dimensions of the samples 120 x 15 x 10 mm3, adapted from the ASTM D3039 standard [43]. From the tensile test, Young's modulus (E), tensile strength (), and ductility (ε) were calculated for all the composites.

2.6. Bending test

The bending test was carried out in the three-point

bending mode using an EMIC machine model DL10000, at the Non-Destructive Testing, Corrosion and Welding Laboratory, Rio de Janeiro, Brazil. The test methodology was in accordance with ASTM D790 [44]. The specimens were made from the composite plates by adapting the standard dimensions to 120 x 15 x 10 mm. Seven samples were used for each composite condition. Other parameters, such as the deformation speed and the distance between the supports were set as 2 mm/min and 4 times the specimens' width, respectively. The flexural results were analyzed in order to obtain both the maximum stress or flexural strength (σmax) and the flexural modulus (E), which were calculated using the Eqs. (1) and (2).

$$\sigma_{max} = \frac{3LQ_m}{2bd^2} \quad (1)$$

$$E = \frac{mL^3}{4bd^3} \quad (2)$$

Where:
Q_m – maximum load, N;
m – slope of the tangent to the initial straight-line portion of the load-deflection curve, N/mm;
L – support span, mm;
b, and d – width of beam tested, mm, and depth of beam tested, mm respectively;

2.7. Transmission electronmicroscopy (TEM)

The morphology and crystalline structure of GNPs were analyzed by high-resolution transmission electron microscopy (HR-TEM) and Selected area electron diffraction (SAED) modes. Analyzes were performed using the JEOL 2100F microscope, at the Brazilian Center for Physical Research (CBPF), Rio de Janeiro, Brazil. The microscope was equipped with a CMOS camera and operated with an accelerating voltage of 200 kV.

2.8. Scanning electron microscopy(SEM)

Microscopic analyses were performed in order to observe the fracture surface of the composites after the tensile tests, as well as the surface morphology of the HDPE and HDPE/GNP nanocomposites films, using a scanning electron microscope (SEM Quanta FEG 250, FEI), operating with secondary electrons accelerated at 10 kV. Samples were sputter coated in a LEICA equipment model EM ACE600, at the CBPF.

2.9. X-ray diffraction (XRD) analysis

XRD analysis was performed to determine the diffraction patterns, as well as estimate the crystallinity fraction of HDPE, HDPE/0.10%GNP, HDPE/0.25%GNP, HDPE/0.50%GNP nanocomposites. The equipment used was a PANalytical X'pert Pro diffractometer. The diffractometer was equipped with a Co (cobalt) anode and scintillation counter type detector (NaI). Operation parameters were set as power 40 mA x 40 kV, sweep from 5° to 75°, in the configuration θ–2θ coupled.

3. RESULTS AND DISCUSSIONS

3.1. TEM analysis

HR-TEM characterization was performed to visualize the morphology of the graphene sheets, as presented in Figure 3a. These sheets have different shapes, and sizes (ranging from micrometers to nanometers); however, they present nanometric layer thicknesses. Some of these sheets are rolled or semi-rolled, as displayed in Figure 3b and c. This is due to the higher thermodynamic stability of the 2D membrane resulting from microscopic crumpling via bending or buckling [45]. The sheet's structure was analyzed by SAED, as shown in Figure 3d, showing well-defined 'monocrystalline-type' spots, which were indexed as ICSD-76767 with the space group P63/mmc. In addition to the sheets, clusters of GNP were also found, Figure 3d, with less than 20 nm in length as shown in Figure 3e. However, all GNP together act as a polycrystalline sheet, which was confirmed by the SAED diffraction pattern in Figure 3f. The integrated angular intensity of the diffraction patterns in Figure 3g shows peaks with maxima at similar interplanar distances to P63/mmc (hexagonal), which are consonant with the ones found in the literature [46-48].

https://doi.org/10.29183/2447-3073.MIX2023.v9.n3.50-65

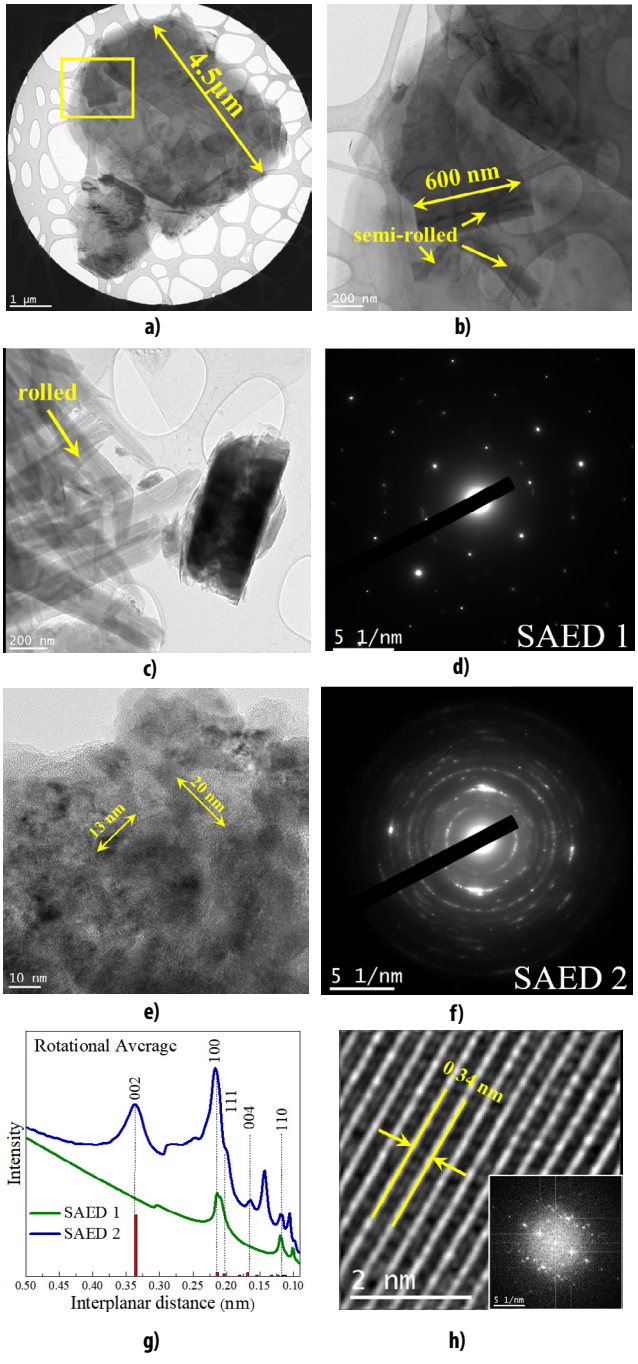

Figure 3: Shows the HR-TEM images of the GNPs

(a) agglomerate of GNPs;

(b) presents the GNP monocrystalline structure semi-rolled;

(c) displays GNP completely rolled;

(d)diffraction pattern of monocrystalline structured GNPs;

(e) agglomerate with nanometric GNPs;

(f) Diffraction pattern of polycrystalline agglomerate;

(g) Intensity profile and interplanar distances of the indexed planes through the diffraction points indicated in the panel of areas.

Fonte: Authors (2023).

As can be seen from Figure 3g, the interplanar distances for the monocrystalline planes {002}, {100}, {111}, {004}, and {110} from SAED were calculated as 0.34, 0.22, 0.20, 0.17, and 0.12 nm, respectively. Figure 3h displays the interplanar distance of 0.34 nm which corresponds to the d-spacing of the {002} planes of GNPs that was further confirmed by the XRD analysis. The diffracted crystal planes registered in XRD ({002}, and {004}) are also confirmed by SAED.

However, Figure 3g shows some unidentified reflections that may have their origin due to the electron wavelength being smaller than the XRD, and causing diffraction at smaller angles, i.e., the multiple scattering in SAED. This is attributed to the interactions of matter with electrons being stronger than with X-rays resulting in reflections in SAED that are not observed in XRD [49,50]. The diffracted crystal planes registered in XRD ({002}, and {004}) are different from the ones identified in SAED {104}, and {015}, except for {100}.

3.2. X-ray diffraction analysis

The crystal structures of GNPs, HDPE, and HDPE/GNP nanocomposites were studied and their XRD patterns are shown in Figure 4. The GNP diffractogram shows a sharp peak at 2θ ≈ 30.69° and weak peaks at 2θ ≈ 51.96°, and 64.18° corresponding to carbon reflections {002}, {100}, and {004}, respectively [36,50]. The sharp peak located at 2θ ≈ 30.69° is characteristic of hexagonal nanoplatelets, with a d-spacing of 0.338 Å, calculated using Braag's law.

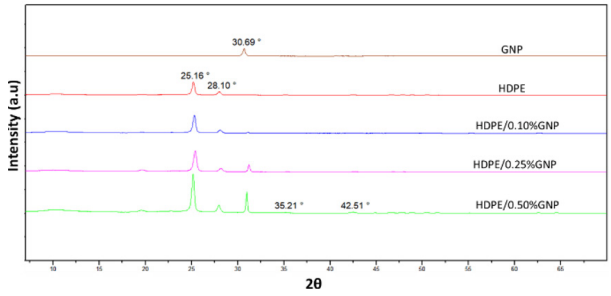

Figure 4: XRD patterns of the HDPE/GNP nanocomposites with different nanofiller loadings.
Source: Authors (2023).

Furthermore, two strong peaks centered at 2θ = 25.16° and 2θ = 28.10°, corresponding to reflections {110} and {200} of the HDPE orthorhombic phase, and two weak peaks centered at 2θ = 35.21° and 42.51°, corresponding to the reflection planes {210} and {020}, respectively, were clearly seen in the plain HDPE XRD pattern [50].

In the XRD patterns of HDPE/GNP nanocomposites, the peak intensities at 2θ ≈ 25.16° and 2θ ≈ 28.10° decreased with increasing GNP load, while the peak intensities at 2θ ≈ 35.21° and 2θ ≈ 42.51° increased. The XRD pattern of HDPE-based nanocomposites exhibited a combination of HDPE and GNP associated peaks.

The crystalline fraction was estimated using the ratio of the area under the crystalline peaks to the total area under the spectrum for each nanocomposite. As a result, the crystallinity fraction increases as the amount of GNP increases, HDPE (57.45%), HDPE/0.10%GNP (58.60%), HDPE/0.25%GNP (60.17%) and HDPE/0.50%GNP (65.43%). Thus, these results indicate that GNPs can act as nucleating agents and that nucleation begins in the vicinity of GNPs [36,42,50].

3.3. Bending test results

Three-points bending tests were carried out on the hot compression molded Jute/HDPE, Jute/HDPE/0.10%GNP, Jute/HDPE/0.25%GNP, and Jute/HDPE/0.50%GNP nanocomposites. Considering the overlap observed in error bars, as shown in Figure 5, it can be inferred that the flexural strength changed very little with the different composite formulations. As a result, an analysis of variance (ANOVA) was conducted using the data of Figure 5, and the discussion is provided below.

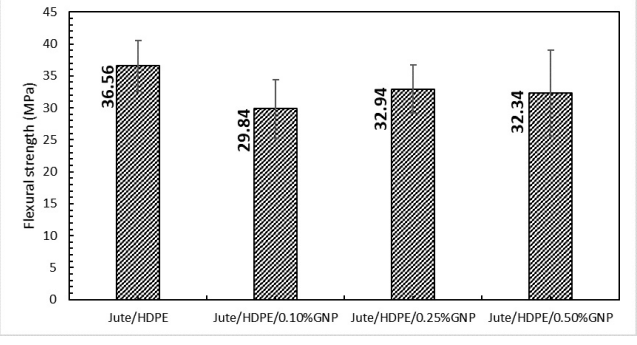

Figure 5: Flexural strength at yield of the nanocomposites with different GNP loadings.
Source: Authors (2023).

From ANOVA, the F-calculated (2.26) is lower than F-critic (3.01); therefore, this result indicates that the average values of flexural strength are equal, with 95% of confidence. However, a significant increase in the flexural modulus with increasing GNP wt.% was found in Figure 6. The Jute/HDPE/0.50%GNP nanocomposite presented a higher elasticity modulus than the other composites investigated in this work. A 65% increase in the elasticity modulus of Jute/HDPE/0.50%GNP nanocomposite was observed, when compared to the Jute/HDPE composite.

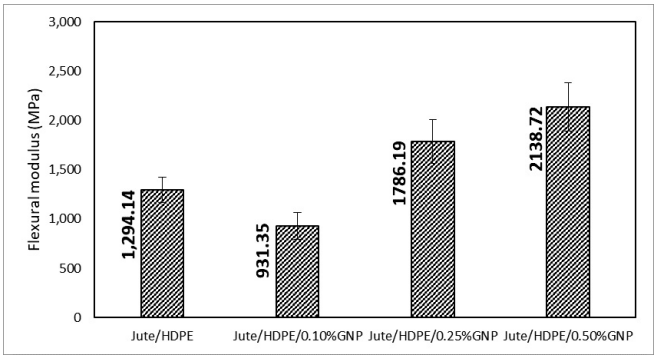

Figure 6: . Flexural modulus of the nanocomposites with different GNP loadings
Source: Authors (2023).

The Tukey test was performed, based on the minimum significant difference (msd), which is a value that can discriminate which treatment shows the difference in its average values. This value can be calculated using Eq. (3). Once the difference between the average values of groups, compared two by two, is higher than the msd value, this pair is considered to be different.

$$msd = q \cdot \sqrt{\frac{ASR}{r}} \qquad (3)$$

where ASR is the average square of the residue inside the groups; r is the number of repetitions of each treatment inside the groups; and q is the total student amplitude (tabulated value), which depends on the degree of freedom (DF) of the residue and the number of treatments.

Then, based on the results shown in Figure 6, ANOVA was performed. With 95% confidence, one can say that the average values are different since F-calculated (39.28) > F-critic (3.24). As a result, the Tukey test was used to determine how groups varied from one another, and the msd was calculated as 387.28. As a direct consequence, the values presented in red in Table 1 are thought to be distinct from their corresponding rows and columns, or vice versa.

Almost all values in Table 1 differ from one another when compared two by two, with the exception of Jute/HDPE/0.10%GNP and Jute/HDPE. Additionally, the Jute/HDPE/0.25%GNP showed a noteworthy rise of 38%. The-

se findings show that the flexural characteristics of the nanocomposite's changed as a result of the melt mixing process of the GNP nanofiller into the HDPE matrix.

	Jute/HDPE	Jute/HDPE /0.10%GNP	Jute/HDPE /0.25%GNP	Jute/HDPE /0.50%GNP
Jute/HDPE	0.00	362.78	492.06	844.59
Jute/HDPE /0.10%GNP	362.78	0.00	854.84	1207.37
Jute/HDPE /0.25%GNP	492.06	854.84	0.00	352.53
Jute/HDPE /0.50%GNP	844.59	1207.37	352.53	0.00

Table 1: Tukey test for the results of Flexural modulus of the nanocomposites. **Source**: Authors (2023).

Furthermore, the Jute/HDPE/0.50%GNP composite's flexural characteristics outperformed those reported in the literature for HDPE nanocomposites with multiple GNP concentrations ranging from 0 to 10 wt%. [28]. According to these findings, thermoplastic matrices combined with NLFs and GNP may provide a brand-new, highly promising class of nanocomposites for use in engineering [28,51].

These findings may be related to the dispersion and aligning of the nanofiller in the HDPE matrix, i.e., the smaller amount of GNPs used in the extrusion and subsequent hot molding of the HDPE/GNP films resulted in less agglomerations and GNPS misalignment in the HDPE films. Therefore, the flexural characteristics tend to increase with the increase in GNP amount since they are scattered perpendicular to the flexural stress [51].

3.4. Tensile test results

Through the tensile tests, the ultimate strength (σu), modulus of elasticity €, ductility (εt), and toughness (T) (area under the σ vs ε curve) were obtained. Figure 7 shows the results for the modulus of elasticity.

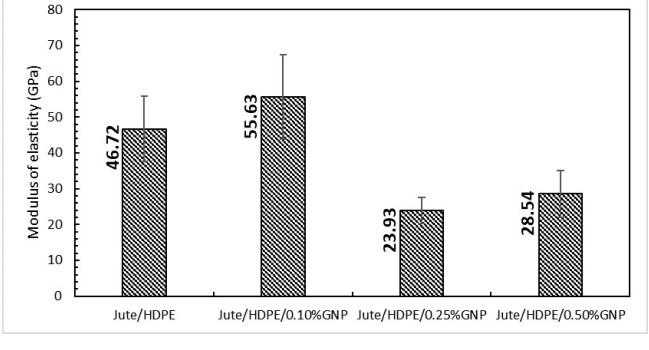

Figure 7: Modulus of elasticity of the nanocomposites with different GNP loadings. **Source:** Author (2023).

As the nanofiller weight fraction increases, the value of E presents a tendency to decrease, as seen in Figure 7. The results from the ANOVA and Tukey tests, to determine if the average values are substantially different from one another, are displayed in Table 2.

Because the F-calculated value (23.73) is higher than the F-critic, it is evident that the average values E are significantly different (3.49). Then, one is able to note that the Jute/HDPE/0.25%GNP and Jute/HDPE/0.50%GNP are distinct from the Jute/HDPE and Jute/HDPE/0.10%GNP based on the Tukey test, with a msd of (1477.88), shown in Table 2.

	Jute/HDPE	Jute/HDPE /0.10%GNP	Jute/HDPE /0.25%GNP	Jute/HDPE /0.50%GNP
Jute/HDPE	0.00	1646.03	1742.13	1271.49
Jute/HDPE /0.10%GNP	1646.03	0.00	3388.16	2917.53
Jute/HDPE /0.25%GNP	1742.13	3388.16	0.00	470.64
Jute/HDPE /0.50%GNP	1271.49	2917.53	470.64	0.00

Table 2: Tukey test for the results of Modulus of elasticity of the nanocomposites. **Source**: Authors (2023).

The increase in GNP fraction caused significant changes in the value of E. For tensile properties, lower amounts of GNP showed to be more efficient at enhancing the mechanical behavior. This phenomenon might be associated with stress concentration points due to the agglomeration of the GPNs in the HDPE matrix [51-53]. However, the values E found for the Jute/HDPE composites (4.27 GPa) were much higher than those reported in the literature (~1.0 GPa) [54,55].

An increase of 50% was shown by the Jute/HDPE/0.10%GNP composite (6.40 GPa) in comparison to the Jute/HDPE composite studied in this work. When compared to the value reported in the literature, the increase becomes 540% [54,55]. Additionally, another noticeable fact was that the value of E for the Jute/HDPE/0.10%GNP composite is similar to that found for the jute composites with thermoset matrices [55].

Regarding the tensile strength, Figure 8 shows the average values and their standard deviation. Because of the overlapped standard deviation bars, the ANOVA and Tukey tests were performed to investigate if the average values present any significant difference.

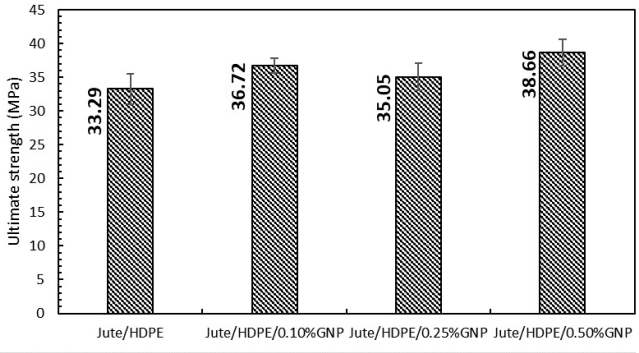

Figure 8: Ultimate strength of the nanocomposites with different GNP loadings.
Source: Author (2023).

From the ANOVA, since F-calculated (9.081) is higher than f-critic (3.098), it was possible to affirm that the average values are not equal with 95% of confidence. Thus, the Tukey test was performed and is presented in Table 3. The msd was calculated as (4.37), which means the Jute/HDPE/0.10%GNP showed a significant difference in relation to the Jute/HDPE composite.

	Jute/HDPE	Jute/HDPE /0.10%GNP	Jute/HDPE /0.25%GNP	Jute/HDPE /0.50%GNP
Jute/HDPE	0.00	3.43	1.77	5.37
Jute/HDPE /0.10%GNP	3.43	0.00	1.66	1.95
Jute/HDPE /0.25%GNP	1.77	1.66	0.00	3.61
Jute/HDPE /0.50%GNP	5.37	1.95	3.61	0.00

Table 3: Tukey test for the results of ultimate strength of the nanocomposites.
Source: Author (2023).

On the other hand, the Jute/HDPE/0.50%GNP and Jute/HDPE/0.10%GNP were considered to be equal, i.e., the average values of ultimate strength did not change with further increments in GNP fractions over 0.10 wt.%. This result indicates that at low nanofiller content, graphene nanoplatelets perform significantly better than in higher amounts due to the agglomeration and alignment of the GNPs in the HDPE matrix [53,56-59].

Regarding the ductility (εt) the results indicate that the higher the amount of GNP in the HDPE matrix, the higher the ductility, as one can see in Figure 9. This could be associated with the voids in the HDPE matrix around the GNPs due to the low compatibility between them, as well as with the agglomeration of the GNP in the HDPE matrix [59]. These features cause a decrease in the GNPs' superficial area, hence the load transmission through the matrix decreases with the increase of added GNP fraction.

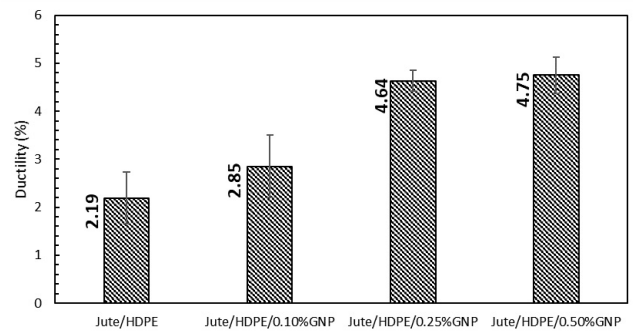

Figure 9: Results of ductility () for the nanocomposites.
Source: Author (2023).

As seen in Figure 9, some relatively higher values of the standard deviation may cast doubt on the possible differences between the average values of the listed properties. In order to evaluate if there was a significant difference between the tensile results, within the groups of each property, the (ANOVA) and Tukey test were performed.

For ductility, F-calculated (43.90) is higher than F-critic (3.10), which guarantees that the average values are different with 95% of confidence. Then, the Tukey test was performed in order to identify what composites presented the most significant difference and the result of the test is presented in Table 4.

	Jute/HDPE	Jute/HDPE /0.10%GNP	Jute/HDPE /0.25%GNP	Jute/HDPE /0.50%GNP
Jute/HDPE	0.00	0.20	0.58	0.49
Jute/HDPE /0.10%GNP	0.20	0.00	0.38	0.29
Jute/HDPE /0.25%GNP	0.58	0.38	0.00	0.09
Jute/HDPE /0.50%GNP	0.49	0.29	0.09	0.00

Table 4: Tukey test for the results of ductility of the nanocomposites.
Source: Authors (2023).

The msd was calculated as 4.45, and then based on Table 4, with a 95% confidence level, the Jute/HDPE/0.50%GNP group is the one exhibiting the highest ductility in Figure 9. Moreover, one should notice that the Jute/HDPE and Jute/HDPE/0.25%GNP formulations also present a significant difference. However, the Jute/HDPE/0.25%GNP and Jute/HDPE/0.50%GNP are considered to be equal in relation to their average ductility values in Figure 9. Similarly, no significant difference is found for the ductility values between Jute/HDPE and Jute/HDPE/0.10%GNP nanocomposites. In

https://doi.org/10.29183/2447-3073.MIX2023.v9.n3.50-65

fact, this means that the GNP in the HDPE matrix does influence the ductility of the nanocomposites.

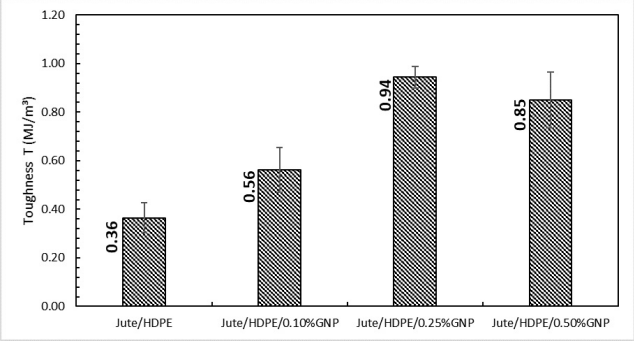

Figure 10: Results of toughness (T) for the nanocomposites.
Source: Authors (2023).

The toughness, as shown in Figure 10, is the energy needed to break the composite, and can be calculated from the area under the stress-strain curve or by the datasheet of the tensile test. One can notice an increase in the toughness with the increase of the GNP amount until 0.25 wt.%. In comparison to the Jute/HDPE (0.36 MJ/m^3), the Jute/HDPE/0.10%GNP (0.56 MJ/m^3) and Jute/HDPE/0.25%GNP (0.94 MJ/m^3) presented significant enhancements of 56% and 161%, respectively. In practical terms, this result indicates that for the formulation of an ideal composite for engineering applications, such as ballistic protection, the amount of GNP has a limit of 0.25 wt.%.

Regarding the ANOVA for the values of toughness, F-calculated (51.86) is higher than F-critic (3.24), which means the average values of toughness cannot be considered equal with 95% of confidence. Consequently, the Tukey test was performed and the msd was calculated as 0.17. From the Tukey test, presented in Table 5, it is possible to affirm that the amount of GNP causes a significant change in the toughness.

	Jute/HDPE	Jute/HDPE /0.10%GNP	Jute/HDPE /0.25%GNP	Jute/HDPE /0.50%GNP
Jute/HDPE	0.00	0.20	0.58	0.49
Jute/HDPE /0.10%GNP	0.20	0.00	0.38	0.29
Jute/HDPE /0.25%GNP	0.58	0.38	0.00	0.09
Jute/HDPE /0.50%GNP	0.49	0.29	0.09	0.00

Table 5: Tukey test for the results of toughness of the nanocomposites.
Source: Authors (2023).

Furthermore, according to Han *et al*., [59], at low fractions (<0.25 wt.%), fillers have much space to disperse and thus can achieve strong interactions with the matrix. Therefore, stress transferring and load sharing between the filler and matrix are improved. While at higher fractions, the fillers become swarming and aggregating so that clustering has a high chance to form. These aggregates act as stress amplifiers and hence cracks can be easily initiated [42].

3.5. SEM analysis

The morphology of HDPE and HDPE/GNP nanocomposite films, as well as the fracture mechanisms of the Jute/HDPE and Jute/HDPE/GNP composites, were observed using SEM analysis. The surface of the HDPE film is smooth, and uniform as shown in Figure 11a. The HDPE/0.10%GNP film, shown in Figure 11b, has some GNP agglomerates that are protected by the HDPE matrix. The HDPE/0.25%GNP and HDPE/0.50%GNP films are depicted in Figure 11c and d, respectively.

The size and quantity of the agglomerate groups grow as the filler content rises, resulting in a drawback between the GNPs' content and their reinforcing function. Additionally, there are no visible spaces between the HDPE matrix and the GNPs, indicating good GNP-polymer melt bonding. For this reason, the state of dispersion in the specimens indicates that a good interaction of the GNPs with the polymer matrix was achieved [60]. According to Figure 11, the surface of nanocomposites becomes rougher as the GNP concentration rises because the GNP aggregates present greater dimensions.

The deformation mechanisms of Jute/HDPE and Jute/HDPE/GNP nanocomposites includes deformation bands, crazing, tearing, fibrillation of the matrix, and fiber rupture. Figure 12 shows the failure surface of Jute/HDPE and Jute/HDPE/GNP nanocomposites after tensile tests.

Figure 12a displays the typical shear band morphology and fracture features of Jute/HDPE. The fracture mechanism for Jute/HDPE composites differs from the Jute/HDPE/GNP nanocomposites. Fibrillation is a part of the tearing process, as seen in Figure 12b, as a result of significant localized plastic deformation. Additionally, SEM micrographs of nanocomposite materials containing 0.10 wt.% GNPs show the presence of voids and the beginning of cracks from these voids. In this case, polymeric fibrils stabilize the

voids [60].

In the fracture mechanism of HDPE nanocomposites filled with GNPs at high filler contents, i.e., > 0.25 wt.%, the percentage of fibrillation and tearing increases with increasing agglomeration diameter. The fracture surfaces of the Jute/HDPE/0.25%GNP and Jute/HDPE/0.50%GNP nanocomposites are shown in Figure 12c and d.

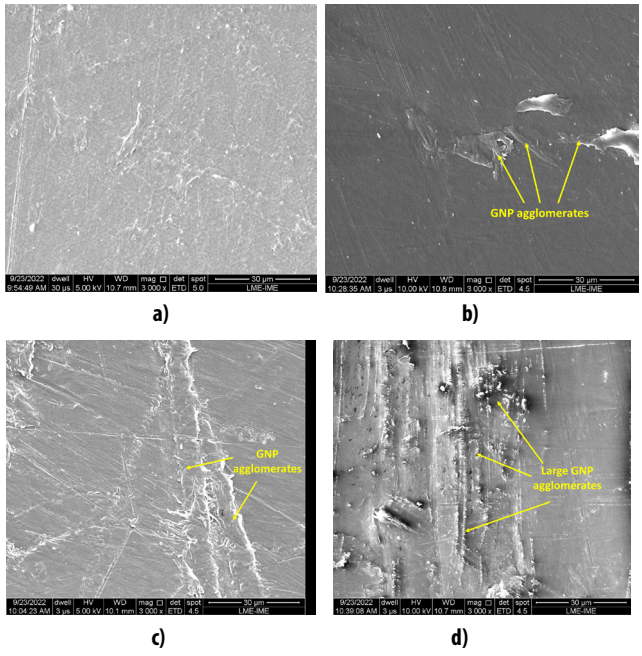

Figure 11: SEM images of surfaces of as-produced.
(a) HDPE, (b) HDPE/0.10%GNP, (c) HDPE/0.25%GNP, and (d) HDPE/0.50%GNP nanocomposite films..
Source: Authors (2023).

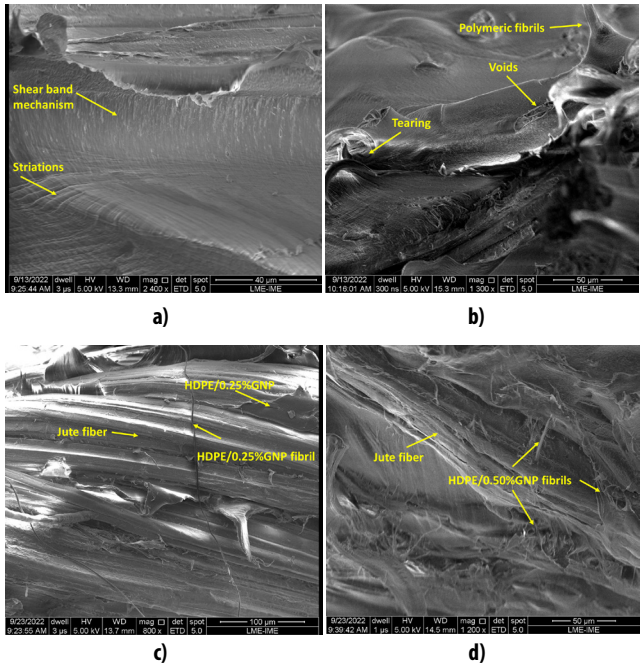

Figure 12: . Fractured specimens of (a) Jute/HDPE, (b) Jute/HDPE/0.10%GNP, (c) Jute/HDPE/0.25%GNP, (d) Jute/HDPE/0.50%GNP.
Source: Authors (2023).

One can see in those figures that the HDPE/GNP matrix was warped in between the jute fabric's fibers. This shows that the HDPE and HDPE/GNP matrices had strong adherence to the jute fabric and filled all gaps between the fabric layers. SEM analysis confirmed that shear banding is the mechanism that governs ductile fracture in Jute/HDPE composites, whereas fibrillation fracture is the mechanism for Jute/HDPE/GNP nanocomposites with larger diameter sizes and GNP contents [60].

CONCLUSIONS

In the present work, the mechanical and flexural performance of novel graphene nanoplatelets (GNP)-reinforced high-density polyethylene nanocomposites reinforced with jute fabric was examined for the first time. In comparison to the Jute/high-density polyethylene (HDPE), the flexural modulus (1,796.19 MPa), ductility (4.64%), and toughness (0.94 MJ/m3) of the Jute/HDPE/0.25%GNP, respectively increased by 38%, 112%, and 161%. Several natural fiber composites with higher GNP contents or thermoset matrices, described in the literature, were found to be inferior in this combination of properties.

The contribution of GNPs was analyzed by XRD, HR--TEM, and SEM, highlighting their structures and morphologies. According to HR-TEM analysis, GNPs are monocrystalline structures that take on a variety of sizes, forms, and configurations when they are aggregated. However, they always exhibit sheet morphologies with nanometric thicknesses. Additionally, the HDPE/GNP films' XRD spectra show that the GNPs perform as a nucleating agent for the crystalline phase of the HDPE matrix.

The fracture mechanisms found in Jute/HDPE composites reveal the characteristic shear band deformation of the HDPE matrix. However, when the content of GNP increases in the matrix, the fracture mechanism changes to a more complex combination of fibrillation with tearing and voids. The results presented herein corroborate the novel Jute/HDPE/0.25%GNP nanocomposite as a promising type of composite for engineering applications.

REFERÊNCIAS

NURAZZI, N. M., ASYRAF, M. R. M., FATIMAH ATHIYAH, S., SHAZLEEN, S. S., RAFIQAH, S. A., HARUSSANI, M. M., ... & KHALINA, A. A review on mechanical performance of hybrid natural fiber polymer composites for structural applications. **Polymers**, 13(13), 2170. 2021.

SATHISH, S., KARTHI, N., PRABHU, L., GOKULKUMAR, S., BALAJI, D., VIGNESHKUMAR, N., ... & DINESH, V. P. A review of natural fiber composites: Extraction methods, chemical treatments and applications. **Materials Today: Proceedings,** 45, 8017-8023. 2021.

MONTEIRO, S. N., LOPES, F. P. D., BARBOSA, A. P., BEVITORI, A. B., SILVA, I. L. A. D., & COSTA, L. L. D. Natural lignocellulosic fibers as engineering materials—an overview. **Metallurgical and Materials Transactions** A, 42(10), 2963-2974. 2011.

KANNAN, G., & THANGARAJU, R. Recent progress on natural lignocellulosic fiber reinforced polymer composites: A review. **Journal of Natural Fibers**, 1-32. 2021.

OKOLIE, J. A., NANDA, S., DALAI, A. K., & KOZINSKI, J. A. Chemistry and specialty industrial applications of lignocellulosic biomass. **Waste and Biomass Valorization**, 12(5), 2145-2169. 2021.

ASYRAF, M. R. M., ISHAK, M. R., NORRRAHIM, M. N. F., NURAZZI, N. M., SHAZLEEN, S. S., ILYAS, R. A., ... & RAZMAN, M. R. Recent advances of thermal properties of sugar palm lignocellulosic fibre reinforced polymer composites. **International journal of biological macromolecules**, 193, 1587-1599. 2021.

RANGAPPA, S. M., SIENGCHIN, S., PARAMESWARANPILLAI, J., JAWAID, M., & OZBAKKALOGLU, T. Lignocellulosic fiber reinforced composites: Progress, performance, properties, applications, and future perspectives. **Polymer Composites,** 43(2), 645-691. 2022.

NAYAK, S., & KUMAR KHUNTIA, S. Development and study of properties of Moringa oleifera fruit fibers/polyethylene terephthalate composites for packaging applications. **Composites Communications**, 15, 113-119. 2019.

YANG, J., CHING, Y. C., & CHUAH, C. H. Applications of lignocellulosic fibers and lignin in bioplastics: A review. **Polymers**, 11(5), 751. 2019.

SINGH, B., & GUPTA, M. Natural fiber composites for building applications. **In Natural fibers, biopolymers, and biocomposites** (pp. 283-313). CRC Press. 2005.

MOHAMMED, L., ANSARI, M. N., PUA, G., JAWAID, M., & ISLAM, M. S. (2015). A review on natural fiber reinforced polymer composite and its applications. **International journal of polymer science**, 2015.

JOSHI, S. V., DRZAL, L. T., MOHANTY, A. K., & ARORA, S. Are natural fiber composites environmentally superior to glass fiber reinforced composites?. **Composites Part A: Applied science and manufacturing**, 35(3), 371-376. 2004.

NURAZZI, N. M., ASYRAF, M. R. M., KHALINA, A., ABDULLAH, N., AISYAH, H. A., RAFIQAH, S. A., ... & SAPUAN, S. M. A review on natural fiber reinforced polymer composite for bullet proof and ballistic applications. **Polymers,** 13(4), 646. 2021.

NAVEEN, J., JAYAKRISHNA, K., HAMEED SULTAN, M. T. B., & AMIR, S. M. M. Ballistic performance of natural fiber based soft and hard body armour-a mini review. **Frontiers in Materials**, 7, 608139. 2020.

COSTA, U. O., NASCIMENTO, L. F. C., GARCIA, J. M., MONTEIRO, S. N., LUZ, F. S. D., PINHEIRO, W. A., & GARCIA FILHO, F. D. C. Effect of graphene oxide coating on natural fiber composite for multilayered ballistic armor. **Polymers,** 11(8), 1356. 2019.

MONTEIRO, S. N., DRELICH, J. W., LOPERA, H. A. C., NASCIMENTO, L. F. C., DA LUZ, F. S., DA SILVA, L. C., ... & BEZERRA, W. B. A. Natural fibers reinforced polymer composites applied in ballistic multilayered armor for personal protection—an overview. Green materials engineering, 33-47. 2019.

GARCIA FILHO, F. C., LUZ, F. S., OLIVEIRA, M. S., BEZERRA, W. B., BARBOSA, J. D., & MONTEIRO, S. N. Influence of rigid brazilian natural fiber arrangements in polymer composites: Energy absorption and ballistic efficiency. Journal of Composites Science, 5(8), 201. 2021.

AMEER, H., AHMAD, S., NAWAB, Y., ALI, Z., & ULLAH, T. Natural fiber–reinforced composites for ballistic protection. In Composite Solutions for Ballistics (pp. 229-248). Woodhe-

ad Publishing. 2021.

GARCIA FILHO, F. D. C., OLIVEIRA, M. S., PEREIRA, A. C., NASCIMENTO, L. F. C., MATHEUS, J. R. G., & MONTEIRO, S. N. Ballistic behavior of epoxy matrix composites reinforced with piassava fiber against high energy ammunition. Journal of Materials Research and Technology, 9(2), 1734-1741. 2020.

SIVA SANKAR, P., & SINGH, S. B. A Review of Natural Fiber Composites for Structural, Infrastructural and Ballistic Applications. Emerging Trends of Advanced Composite Materials in Structural Applications, 353-373. 2021.

GOWDA, T. M., NAIDU, A. C. B., & CHHAYA, R. Some mechanical properties of untreated jute fabric-reinforced polyester composites. Composites Part A: applied science and manufacturing, 30(3), 277-284. 1999.

HONAKER, K., VAUTARD, F., & DRZAL, L. T. Investigating the mechanical and barrier properties to oxygen and fuel of high density polyethylene–graphene nanoplatelet composites. Materials Science and Engineering: B, 216, 23-30. 2017.

WANG, Y., LIU, X., SHI, Z., LIN, Y., YANG, Y., YANG, Q., ... & LAN, T. Rheological Behavior of High Density Polyethylene (HDPE) Filled with Corn Stalk Biochar. ChemistrySelect, 6(38), 10418-10428. 2021.

AJI, I. S., ZAINUDIN, E. S., KHALINA, A., SAPUAN, S. M., & KHAIRUL, M. D. Studying the effect of fiber size and fiber loading on the mechanical properties of hybridized kenaf/PALF-reinforced HDPE composite. Journal of Reinforced Plastics and Composites, 30(6), 546-553. 2011.

SALLEH, F. M., HASSAN, A., YAHYA, R., & AZZAHARI, A. D. Effects of extrusion temperature on the rheological, dynamic mechanical and tensile properties of kenaf fiber/HDPE composites. Composites Part B: Engineering, 58, 259-266. 2014.

EL-ZAYAT, M. M., ABDEL-HAKIM, A., & MOHAMED, M. A. Effect of gamma radiation on the physico mechanical properties of recycled HDPE/modified sugarcane bagasse composite. Journal of Macromolecular Science, Part A, 56(2), 127-135. 2019.

VASU, A., REDDY, C., DANABOYINA, S., MANCHALA, G., & CHAVALI, M. The Improvement in mechanical properties of coconut shell powder as filter in HDPE composites. J. Polym. Sci. Appl, 1(2), 2-7. 2017.

CHANDEKAR, H., CHAUDHARI, V., & WAIGAONKAR, S. A review of jute fiber reinforced polymer composites. Materials Today: Proceedings, 26, 2079-2082. 2020.

SONG, H., LIU, J., HE, K., & AHMAD, W. A comprehensive overview of jute fiber reinforced cementitious composites. Case Studies in Construction Materials, 15, e00724. 2021.

GOGNA, E., KUMAR, R., SAHOO, A. K., & PANDA, A. A comprehensive review on jute fiber reinforced composites. Advances in industrial and production engineering, 459-467. 2019.

SINGH, H., SINGH, J. I. P., SINGH, S., DHAWAN, V., & TIWARI, S. K. A brief review of jute fibre and its composites. Materials Today: Proceedings, 5(14), 28427-28437. 2018.

YASHAS GOWDA, T. G., SANJAY, M. R., SUBRAHMANYA BHAT, K., MADHU, P., SENTHAMARAIKANNAN, P., & YOGESHA, B. Polymer matrix-natural fiber composites: An overview. Cogent Engineering, 5(1), 1446667. 2018.

KHAN, M. A., RAHAMAN, M. S., AL-JUBAYER, A., & ISLAM, J. M. M. Modification of jute fibers by radiation-induced graft copolymerization and their applications. Cellulose-Based Graft Copolymers: Structure and Chemistry; Thakur, VK, Ed, 209-235. 2015.

HUSSAIN, S. A., PANDURANGADU, V., & PALANIKUAMR, K. Mechanical properties of green coconut fiber reinforced HDPE polymer composite. International Journal of Engineering Science and Technology, 3(11), 7942-7952. 2011.

GENG, Y., WANG, S. J., & KIM, J. K. Preparation of graphite nanoplatelets and graphene sheets. Journal of colloid and interface science, 336(2), 592-598. 2009.

EVGIN, T., TURGUT, A., HAMAOUI, G., SPITALSKY, Z., HORNY, N., MICUSIK, M., ... & OMASTOVA, M. Size effects of graphene nanoplatelets on the properties of high-density polyethylene nanocomposites: morphological, thermal, electrical, and mechanical characterization. Beilstein journal of nanotechnology, 11(1), 167-179. 2020.

HOPE, J. T., SUN, W., KEWALRAMANI, S., SAHA, S., LAKHE, P., SHAH, S. A., ... & HULE, R. A. Scalable production of graphene nanoplatelets for energy storage. ACS Applied Nano Materials, 3(10), 10303-10309. 2020.

JEON, I. Y., BAE, S. Y., SEO, J. M., & BAEK, J. B. Scalable production of edge-functionalized graphene nanoplatelets via mechanochemical ball-milling. Advanced Functional Materials, 25(45), 6961-6975. 2015.

LI, B., & ZHONG, W. H. Review on polymer/graphite nanoplatelet nanocomposites. Journal of materials science, 46(17), 5595-5614. 2011.

CATALDI, P., ATHANASSIOU, A., & BAYER, I. S. Graphene nanoplatelets-based advanced materials and recent progress in sustainable applications. Applied Sciences, 8(9), 1438. 2018.

ESCOCIO, V. A., VISCONTE, L. L., CAVALCANTE, A. D. P., FURTADO, A. M. S., & PACHECO, E. B. Study of mechanical and morphological properties of bio-based polyethylene (HDPE) and sponge-gourds (Luffa-cylindrica) agroresidue composites. In AIP Conference Proceedings (Vol. 1664, No. 1, p. 060012). AIP Publishing LLC. 2015.

TOMASI TESSARI, B., VARGAS, N., RODRIGUES DIAS, R., MIRANDA PEREIRA, I., ROSSA BELTRAMI, L. V., LAVORATTI, A., ... & ZATTERA, A. J. Influence of the addition of graphene nanoplatelets on the ballistic properties of HDPE/aramid multi-laminar composites. Polymer-Plastics Technology and Materials, 61(4), 363-373. 2022.

ASTM International. Standard Test Method for Tensile Properties of Polymer Matrix Composite Materials; D3039/D3039M – 17; ASTM International: West Conshohocken, PA, USA. 2017.

ASTM International. Standard Test Methods for Flexural Properties of Unreinforced and Reinforced Plasticsand Electrical Insulating Materials; D790 – 17; ASTM International: West Conshohocken, PA, USA. 2017.

WANG, G., YANG, J., PARK, J., GOU, X., WANG, B., LIU, H., & YAO, J. Facile synthesis and characterization of graphene nanosheets. The Journal of Physical Chemistry C, 112(22), 8192-8195. 2008.

SUJITH, R., CHAUHAN, P. K., GANGADHAR, J., & MAHESHWARI, A. Graphene nanoplatelets as nanofillers in mesoporous silicon oxycarbide polymer derived ceramics. Scientific reports, 8(1), 1-9. 2018.

ARMUGAM, A., HOSAKOPPA S, N., & HOLAVANAHALLI DORAISWAMY, S. Enhanced corrosion resistance of atmospheric plasma-sprayed zirconia–GNP composite by graphene oxide nanoplatelet encapsulation. Applied Physics A, 126(8), 1-12. 2020.

WANG, F., & DRZAL, L. T. Development of stiff, tough and conductive composites by the addition of graphene nanoplatelets to polyethersulfone/epoxy composites. Materials, 11(11), 2137. 2018.

GUERRA, V., WAN, C., DEGIRMENCI, V., SLOAN, J., PRESVYTIS, D., WATSON, M., & MCNALLY, T. Characterisation of graphite nanoplatelets (GNP) prepared at scale by high-pressure homogenisation. Journal of Materials Chemistry C, 7(21), 6383-6390. 2019.

XIANG, D., WANG, L., TANG, Y., ZHAO, C., HARKIN-JONES, E., & LI, Y. Effect of phase transitions on the electrical properties of polymer/carbon nanotube and polymer/graphene nanoplatelet composites with different conductive network structures. Polymer International, 67(2), 227-235. 2018.

HONAKER, K., VAUTARD, F., & DRZAL, L. T. Influence of processing methods on the mechanical and barrier properties of HDPE-GNP nanocomposites. Advanced Composites and Hybrid Materials, 4(3), 492-504. 2021.

SARKER, F., KARIM, N., AFROJ, S., KONCHERRY, V., NOVOSELOV, K. S., & POTLURI, P. High-performance graphene-based natural fiber composites. ACS applied materials & interfaces, 10(40), 34502-34512. 2018.

PAPAGEORGIOU, D. G., KINLOCH, I. A., & YOUNG, R. J. Mechanical properties of graphene and graphene-based nanocomposites. Progress in Materials Science, 90, 75-127. 2017.

MOHANTY, S., & NAYAK, S. K. Mechanical and rheological characterization of treated jute-HDPE composites with a different morphology. Journal of Reinforced Plastics and Composites, 25(13), 1419-1439. 2006.

GUPTA, M. K., SRIVASTAVA, R. K., & BISARIA, H. Potential of

jute fibre reinforced polymer composites: a review. Int. J. Fiber Text. Res, 5(3), 30-38. 2015.

RAFIEE, M. A., RAFIEE, J., WANG, Z., SONG, H., YU, Z. Z., & KORATKAR, N. Enhanced mechanical properties of nanocomposites at low graphene content. ACS nano, 3(12), 3884-3890. 2009.

SHEN, X. J., LIU, Y., XIAO, H. M., FENG, Q. P., YU, Z. Z., & FU, S. Y. The reinforcing effect of graphene nanosheets on the cryogenic mechanical properties of epoxy resins. Composites Science and Technology, 72(13), 1581-1587. 2012.

CHIENG, B. W., IBRAHIM, N. A., WAN YUNUS, W. M. Z., HUSSEIN, M. Z., & LOO, Y. Y. Effect of graphene nanoplatelets as nanofiller in plasticized poly (lactic acid) nanocomposites. Journal of Thermal Analysis and Calorimetry, 118(3), 1551-1559. 2014.

HAN, S., MENG, Q., QIU, Z., OSMAN, A., CAI, R., YU, Y., ... & ARABY, S. Mechanical, toughness and thermal properties of 2D material-reinforced epoxy composites. Polymer, 184, 121884. 2019.

TARANI, E., CHRYSAFI, I., KÁLLAY-MENYHÁRD, A., PAVLIDOU, E., KEHAGIAS, T., BIKIARIS, D. N., ... & CHRISSAFIS, K. Influence of graphene platelet aspect ratio on the mechanical properties of HDPE nanocomposites: Microscopic observation and micromechanical modeling. Polymers. 12(8). 2020.

Record of authorship contribution:

CRediT Taxonomy (http://credit.niso.org/)

Conceptualization, data curation, investigations, and methodology, U.O.C. and L.F.C.N.;

Formal analysis, validation, writing—original draft preparation, writing—review and editing, U.O.C. and S.N.M.;

Testing preparation, data analysis, writing—paper, U.O.C. and L.F.C.N.;

Performance of tests, N.R.C.H. and U.O.C.;

Formal analysis validation and visualization, W.B.A.B. and W.A.P.;

Funding acquisition, writing review, and editing, S.N.M.

All authors have read and agreed to the published version of the manuscript.

FUNDING
This research received no external funding.

CONFLICTS OF INTEREST
The authors declare no conflict of interest.

ACKNOWLEDGMENTS
The authors would like to thank the support to this investigation by the Brazilian agencies: CNPq, CAPES and FAPERJ. As well as the UCSGraphene for providing the Graphene nanoplatelets.

DATA AVAILABILITY STATEMENT
All data underlying the results are available as part of the article and no additional source data are required.

AUTHORS

Orcid: 0000-0002-3844-1536
ULISSES OLIVEIRA COSTA, Master | Military Institute of Engineering - IME| Materials Science | Rio de Janeiro, Rio de janeiro (RJ) - Brazil | Correspondence to: (Praça Gen. Tibúrcio, 80, Urca, Rio de Janeiro-RJ, 22290-270) | E-maill: ulissesolie@ime.eb.br

Orcid: 0000-0002-5463-7299
WENDELL BRUNO ALMEIDA BEZERRA, Doctor | Military Institute of Engineering - IME| Materials Science | Rio de Janeiro, Rio de janeiro (RJ) - Brazil | Correspondence to: (Praça Gen. Tibúrcio, 80, Urca, Rio de Janeiro-RJ, 22290-270) | E-maill: wendellbez@gmail.com

Orcid: 0000-0002-8898-2584
NOEMI RAQUEL CHECCA HUAMAN, Doctor | Brazilian Center for Physics Research, CBPF | Eletronic Microscopy | Rio de Janeiro, Rio de janeiro (RJ) - Brasil | Correspondence to: (Dr. Xavier Sigaud, 150, Urca, Rio de Janeiro-RJ, 22290-180) | E-maill: noemiraquelchecca@gmail.com

Orcid: 0000-0003-1208-1234
SERGIO NEVES MONTEIRO, PhD | Military Institute of Engineering - IME| Materials Science | Rio de Janeiro, Rio de janeiro (RJ) - Brazil | Correspondence to: (Praça Gen. Tibúrcio, 80, Urca, Rio de Janeiro-RJ, 22290-270) | E-maill:

snevesmonteiro@gmail.com

Orcid: 0000-0003-0560-528X
WAGNER ANACLETO PINHEIRO, Doctor | Military Institute of Engineering - IME| Materials Science | Rio de Janeiro, Rio de janeiro (RJ) - Brazil | Correspondence to: (Praça Gen. Tibúrcio, 80, Urca, Rio de Janeiro-RJ, 22290-270) | E-maill: anacleto@ime.eb.br

Orcid: 0000-0003-0560-528X
LUCIO FABIO CASSIANO NASCIMENTO, Doctor | Military Institute of Engineering - IME| Materials Science | Rio de Janeiro, Rio de janeiro (RJ) - Brazil | Correspondence to: (Praça Gen. Tibúrcio, 80, Urca, Rio de Janeiro-RJ, 22290-270) | E-maill: lucio@ime.eb.br

HOW TO CITE THIS ARTICLE

COSTA, Ulisses Oliveira; BEZERRA, Wendell Bruno Almeida; HUAMAN, Noemi Raquel Checca; MONTEIRO, Sergio Neves; PINHEIRO, Wagner Anacleto; NASCIMENTO, Lucio Fabio Cassiano. Mechanical Behavior Of High-density Polyethylene Reinforced With Graphene Nanoplatelets And Jute Fabric. **MIX Sustentável,** [S.l.], v. 9, n. 3, p. 50-65, julho. 2023. ISSN 24473073. Disponível em:<http://www.nexos.ufsc.br/index.php/mixsustentavel>. Acesso em: dia mês. ano. doi:https://doi.org/10.29183/2447-3073.MIX2023.v9.n3.50-65.

SUBJECTED IN: 31/12/2022
ACCEPTED IN: 25/03/2023
PUBLISHED IN: XX/07/2023
RESPONSIBLE EDITORS: Aguinaldo dos Santos e Paulo Cesar Machado Ferroli